We are IntechOpen, the world's leading publisher of Open Access books Built by scientists, for scientists

6,900
Open access books available

185,000
International authors and editors

200M
Downloads

Our authors are among the

154
Countries delivered to

TOP 1%
most cited scientists

12.2%
Contributors from top 500 universities



WEB OF SCIENCE™

Selection of our books indexed in the Book Citation Index in Web of Science™ Core Collection (BKCI)

Interested in publishing with us?
Contact book.department@intechopen.com

Numbers displayed above are based on latest data collected.
For more information visit www.intechopen.com



Chapter 8

Interaction Between Aerosol Particles and Maritime Convective Clouds: Measurements in ITCZ During the EPIC 2001 Project

J.C. Jiménez-Escalona and O. Peralta

Additional information is available at the end of the chapter

http://dx.doi.org/10.5772/50249

1. Introduction

Atmospheric particles interact directly with solar radiation extinguishing part of it and decreasing the amount of radiation that reaches the Earth's surface. This effect produces a change in the local radiative balance. On the other hand, it also presents an indirect effect on the interaction with radiation because these particles are an important element in the formation and development of clouds influencing their optical properties and the length of residence.

There are studies that have focused primarily on understanding and explaining the role of atmospheric particles in the formation and evolution of clouds. They have shown enough information able to explain those processes in theory (e.g. Pruppacher and Klett, 1997). And they have been validated with experimental works (e.g. Twomey, 1991; Raga and Jonas, 1993 a, b).

However, other issues of importance that do not yet have much information are the processes that modify the properties of atmospheric particles interacting with the cloud and the effects of changes in the environment. Particles increase their average size in regions of high relative humidity (RH) near the clouds (Baumgardner et al, 1996; Baumgardner and Clarke, 1998). Other studies show that the clouds condensation nuclei (CCN) are relatively higher in regions where a cloud is evaporated compared with places without clouds (DeFelice and Saxena, 1994; DeFelice and Cheng, 1998; Naoki et al, 2001). Also, the composition of atmospheric particles may change resulting from chemical reaction in aqueous state (Hegg et al, 1980; O'Dowd et al, 2000, Alfonso and Raga, 2002). Aerosol particles used as CCN show an increase in size after the cloud drops are evaporated (Hobbs, 1993). Towmey (1974) and Albrecht (1989) showed that changes in particles concentrations

INTECH
open science | open minds

© 2012 Jiménez-Escalona and Peralta, licensee InTech. This is an open access chapter distributed under the terms of the Creative Commons Attribution License (http://creativecommons.org/licenses/by/3.0), which permits unrestricted use, distribution, and reproduction in any medium, provided the original work is properly cited.

in an area influenced by polluted sources modify the local cloud albedo and its life time, inhibiting the rain process (Rosenfeld, 1999).

So, there are many processes that change the properties of atmospheric particles and their interactions with clouds. This chapter is focused on identifying and assessing the main processes involved with particles in the vicinity of maritime convective clouds at the Inter-Tropical Convergence Zone (ITCZ).

1.1. Clouds in the Inter-Tropical Convergence Zone (ITCZ)

The ITCZ is one of the most important weather systems in the Tropics. The area shows a decisive influence on the characterization of different clime and weather conditions in tropical region. The ITCZ is characterized by several interactions between the ocean and the atmosphere, identified as:

- Area of confluence of trade winds from the Northeast and Southeast.
- Area where the Equatorial depression is located due to an increased incidence of solar radiation and the presence of convective phenomena.
- Area of maximum temperature on the sea surface
- Maximum mass convergence zone
- Area that has the band of maximum coverage of convective clouds.

Therefore, the ITCZ is represented as a line of clouds of deep convection extending across the Atlantic and Pacific oceans, located between the 5° and 10° N (Holton, 1992). The band moves depending on the season, always matching in areas with high solar intensity or where the sea surface has higher temperatures. The clouds movement is towards the Southern hemisphere between September and February, and in the opposite direction in the next few months until the end of the summer in the Northern Hemisphere. However, just at the north of the Ecuador, the ITCZ movements are lower (Wallace and Hobbs, 1977). In those areas, the rain intensifies with solar heating. An exception occurs with El Niño-Southern Oscillation (ENSO), and the ITCZ is deflected towards where the ocean surface increases its temperature. A special feature of the region is the presence of a warm water pool, nearby the coast of Mexico, located in the ITCZ between 12° and 8° N from September to November. The presence of high temperatures at the ocean surface promotes a greater amount of moisture and increases convection effects, which result in larger vertical clouds.

1.2. Development of convective clouds

A convective cloud is formed when a mass of moist air acquires buoyancy due to the increase in surrounding temperature; with this process, the presence of atmospheric instability helps to lift the air masses.

Once the air mass reaches the saturation point, water vapor condenses on the CCN. The change of physical state releases latent heat that is absorbed by the air increasing the

buoyancy forces. From now on, the cloud experiences a violent vertical development reaching the maximum height generated by the strong temperature gradient between the cloud core and the environment surrounds it. However, the growing process will be affected by dry air entrainment on the cloud's side walls, inhibiting the vertical development of convective cloud (Squires, 1958; Emanuel, 1982).

The air entrainment dilutes and evaporates droplets releasing aerosol particles, which served as CCN, back into the atmosphere and cooling the air surrounding. The process generates downward movements in the cloud and promotes a high turbulence that mixes the air masses.

1.3. Interaction of atmospheric particles with solar radiation

Atmospheric particles play a very important role in the climate system. Their effects on the direct radiative forcing scattering or absorbing sunlight, and facilitating indirectly the formation of clouds are a relevant object of study since there is no adequate knowledge of their significance on clouds creation. Particles radiative forcing is globally comparable to greenhouse gases, but in the opposite direction because it causes a cooling climate (Charlson et al, 1992). Coakley and Grams (1976) consider that particles between the range $0.05 < r < 1$ μm may cause a cooling surface. Research has shown that the radiative forcing of atmospheric particles depends on their composition, size and altitude (Hansen et al, 1980; Pollack et al, 1981). So, it may be considered that a change in one or several properties on the atmospheric particles might affect the local forcing.

The indirect radiative forcing occurs when the aerosol particles are used as CCN creating cloud droplets. The effects are classified in two types:

a. Radiative forcing induced by an increase of anthropogenic particles promoting a higher concentration of droplets that change the cloud's albedo (Twomey, 1974). This effect is also known as the cloud's albedo or Twomey effects.
b. Radiative forcing caused by a higher concentration of anthropogenic particles, causing a decrease in the droplets diameter and more competition for the water vapor available in the atmosphere. This will reduce the precipitation efficiency and modify the cloud's residence time in the atmosphere (Albrecht, 1989). The event is known as cloud lifetime or Albrecht effects.

1.4. EPIC 2001

East Pacific Investigation of Climate Processes in the Coupled Ocean-Atmosphere System 2001 (EPIC 2001) was sponsored by The U.S. Climate Variability and Predictability Research Program (CLIVAR), which has the goal of providing the observational basis needed to improve the representation of certain key physical processes in coupled ocean atmosphere models. In addition to physical processes, EPIC 2001 research was directed toward a better understanding and simulation of the effects of short-term variability in the east Pacific on climate. This variability is particularly important in the region because conditions in the

ITCZ are highly variable on daily to intra-seasonal time scales. The effects of such variability rectify strongly onto climate time scales in this region.

EPIC 2001 was conceived as an intensive process study along and near 95ºW during September and October 2001. This longitude was chosen to coincide with the Tropical Atmosphere Ocean project (TAO) mooring array in order to provide an overlap between the process study and long-term monitoring.

In addition to the TAO moorings, two aircrafts, the National Center for Atmospheric Research's (NCAR) C-130 and NOAA's P-3, plus two ships, NOAA's R/V Ron H. Brown and the National Science Foundation's (NSF's) R/V New Horizon, and Galapagos-based soundings, were used to make measurements of the atmosphere and ocean in this region. The aircraft were based from 1 September to 10 October 2001 in Huatulco, Mexico. The ships spent approximately 3 weeks in the vicinity of 10º N, 95º W, and then traversed the 95º W line to the equator. After a short stop in the Galapagos Islands, the Ron H. Brown then proceeded south along 95º W and then to the Woods Hole Oceanographic Institute Improved Meteorological Recorder (IMET) mooring at 20º S, 85º W. Meanwhile the New Horizon reversed its track along 95º W and then returned to port.

2. Methodology

On this study we use a P-3 aircraft belonging to the National Oceanic and Atmospheric Administration (NOAA) and a C-130 Hercules property of the National Science Foundation (NSF) operated by the National Center of Atmospheric Research (NCAR). El Centro de Ciencias de la Atmósfera, at the Universidad Nacional Autónoma de México, (UNAM) installed and operated instrumental at the C-130 to measure some properties of atmospheric particles.

2.1. Instrumentation

We used instruments to measure the physical properties of atmospheric particles. The particles chemical composition is inferred from their optical properties as it is explained later in this chapter. Since the atmospheric particles are micro and sub-micron range sizes, the number of particles per volume may provide information on their origin or formation and might infer possible causes about their changes in concentrations.

We use optical counters to estimate the concentration of particles. Their operating principle is based on the extinction of a beam of known wavelength, having gone through an air sample with a certain amount of particles. Table 1 contains the technical details of the instruments used in the EPIC 2001 flights for the study.

2.1.1. Optical counters

Condensation nuclei particle counter (TSI-3760) is an instrument that increases the size of the particles with a forced growth in an environment artificially saturated with butanol. This increases the efficiency of detection and counting of very small droplets (Twomey, 1991).

Instrument type	Parameter	Range	Accuracy
CN counter (TSI Model 3760)	Light-Absorption Coefficient	10^{-7} to 10^{-2} m^{-1}	±5%
PCASP-100X	Light-scattering Coefficient	$1.0x10^{-7}$ to $10x10^{-3}$ m^{-1}	±5%
PMS Model FSSP-300	Number concentration of aerosol	0.01 to > 3 μm 0 to $2x10^{4}$ cm^{-3}	Varies with concentration, about 6% at 3300 cm^{-3}.
	Size spectra of aerosols	0.12 to 3.0 mm (15 channels)	± 20% (Diameter) ±16% (Concentration)
PMS Model FSSP-100	Size spectra of aerosols	0.3 to 20 mm (30 channels)	± 20% (Diameter) ±16% (Concentration)
CCN Counter	Size spectra of aerosols and cloud droplets	2 to 47 mm (30 channels)	± 20% (Diameter) ±16% (Concentration)
	Number concentration of CCN	0.2 to 1.0 % supersaturation	10% at 1% supersaturation

Table 1. Aerosol and cloud particle instrumentation on the C130 aircraft

The CCN is a subset of the total concentration of particles, which can form droplets in an environments of over-saturation, as in a cloud (101 - 110% SS). The CCN counter model 100, determines the concentrations of these atmospheric particles. The operating principle is based on measuring the variation within a thermal gradient diffusion chamber, to create an environment of over-saturation. An electrical system controls the temperature of two plates that create the conditions of over saturation. A beam of laser light passes through the chamber and the instrument measures the amount of light scattered and estimates the concentration of CCN per volume. Delene et al (1998) and Delene and Deshler (2000) have a more detailed description and analysis of this instrument operation.

The PCASP, FSSP300, and FSSP100 provide information on particle concentrations in size defined ranges. The instruments pass a beam of light with specific wavelength and intensity, through the air sample. The particles in the sample scatter the light beam with an intensity that depends on their size, shape and composition. The instrument measures the amount of light scattered with sensors. By knowing the intensity of scattered light and particles composition (water for FSSP100 and FSSP300) or sodium chloride (for PCASP), it is possible to infer the size range of particles to which they belong. A more detailed description of the operation and measurement uncertainty associated with the PCASP can be obtained on Strapp et al (1992).

2.1.2. Instruments location

The external instruments are installed in a pod on the wing and internal within the fuselage in the cabin. The location characterizes the way that each machine takes the air sample to analyze. The external instruments are in direct contact with the air all the time. Thus, the air sampling is instantaneous. But the internal instruments take the air sample by an air inlet and a section of hose that transports it to the device. In this case, the instrument uses a

suction pump to enter the air. The path that the air sample covers must be considered when comparing the data from internal and external instruments. For instance, the CN counter readings show a 1 second delay compared with those obtained instantaneously from the PCASP and the FSSP.

2.2. Composition of atmospheric particles derived by their physical properties

To calculate the particles size we used Mie's theory. It says that the intensity of light scattered in all directions depends on the size and composition of the particle and the wavelength of incident light. Mie's theory considers spherical particles, so the optical counters used this assumption to obtain a value about the size of atmospheric particles.

A particle exposed to a beam of light will eliminate some of the energy that hits on it. This phenomenon of extinction is given by the combination of absorption and scattering of light. Water droplets do not absorb radiation and only scatters light. With this justification, we assume that the dispersion coefficient values are a good approximation to the extinction coefficient of particles.

The amount of light scattered by a particle depends on three combined effects: 1) reflection, 2) refraction and 3) diffraction. Refraction depends on the composition of the particle, while the diffraction depends on the wavelength of incident light, the size, and the shape of the particle. Optical counters use these concepts to calculate the size of particles in an air sample. With this information it is possible to characterize the particles counted in certain size ranges, obtaining the size distribution spectrum of particles.

The instruments are calibrated using refraction indexes for water (1.33), ammonium sulphate (1.48) or sodium chloride particles (1.54). Figure 1 shows the dispersion efficiency depending on the particles diameter with the three refraction indexes from Mie's theory.

Figure 1 shows the sensitivity of dispersion efficiency by varying the composition of particles. If we consider a particle with 0.4 μm diameter, the changes on its composition from water (n = 1.33) to sodium chloride (n = 1.58) is approximately 30 times. This indicates that the difference in the amount of light scattered by a cloud droplet and a NaCl particle increases by several orders of magnitude.

The coefficient of dispersion of a population of particles with size r_0 to r_n is defined by

$$\sigma_s = \int_{r_0}^{r_n} Q_s(\eta, r, \lambda)\pi r^2 n(r)dr \quad (1)$$

where Qs is the scattering efficiency, which is a function of refractive index (η) radius of the particle (r) and the wavelength of scattered light (λ). And n(r) represents the concentration of a population of particles according to radius r.

$$\sigma_s = \sum_{i=1}^{n} Q_s(\eta, r_i, \lambda)\pi r_i^2 n(r_i)dr \quad (2)$$

With this equation and the data obtained by particle counters we calculated the particles dispersion coefficients for the vicinity of the clouds. We used 28 different refractive indexes,

ranging from 1.33 to 1.60, resulting in a matrix of 28 dispersion coefficients for each data. The values were compared against the dispersion coefficients obtained directly from a nephelometer, inferring the approximate refractive index and a possible particles composition.

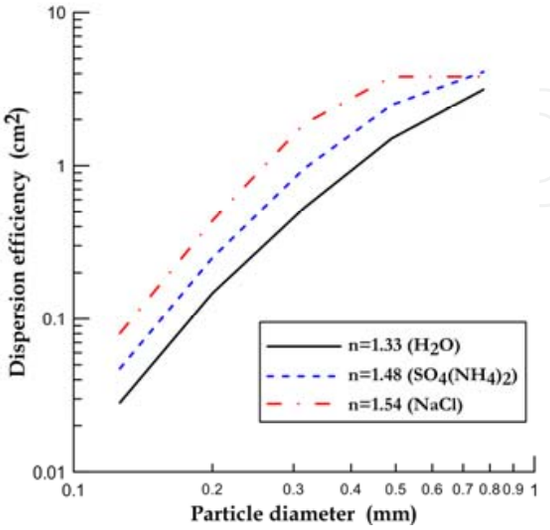


Figure 1. Dispersion efficiency and particle diameter for three different refractive indexes

2.3. Sampling

In EPIC 2001 project we did 19 flights to investigate the ocean-atmosphere interaction, and clouds and aerosol particles properties in the Eastern Pacific. Nine flights were conducted within the ITCZ. The flights were in the area between 8° - 12° North latitude, and 93° - 97° West longitude (figure 2). During the flights were searched and selected young convective and precipitation clouds.

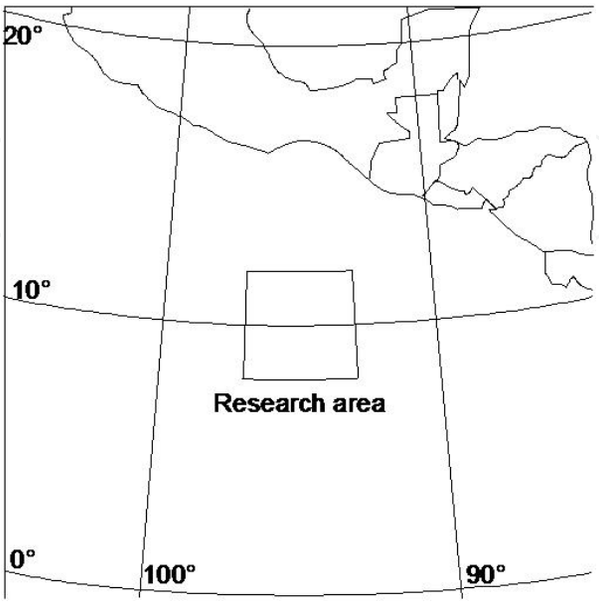


Figure 2. EPIC 2001 research area.

3. Particles processing by clouds

If a mass of moist air is forced to raise it creates a cloud, either by buoyancy promoted by surface heating or by mechanical means, such as climbing up a slope pushed by the wind. When the mass of air containing water vapor is cooled by adiabatic ascent, the vapor pressure increases until it reaches the complete saturation (RH = 100%). The increase in RH results in the formation of cloud droplets, because some particles act as CCN. The particles grow by molecular diffusion to the drop and form a solution. New droplets can interact with interstitial particles in the cloud or collide and coalesce with other droplets changing its composition. If the water droplet evaporates, then releases an aerosol particle with different mass and composition than the original particle. The particle is physical, chemical and hygroscopic different. According to the Köhler curve, a particle increasing its mass may trigger saturation values lower than a smaller particle (Pruppacher and Klett, 1997). In other words, the atmospheric particles that are processed by clouds acquire properties to become more efficient CCN. In addition, the size distribution of particles is modified and can directly influence the evolution of the cloud. The processes change the physical and chemical characteristics of particles, but their concentrations can be identified by analyzing the shapes of the distributions of sizes.

3.1. Particles sizes distribution

Atmospheric particles have different origins; some are from natural sources such as oceans, volcanoes, soil, pollen, forest fires, and so on. And human activities also generate particles that reach the atmosphere. Motor vehicles, power generation, industrial boilers and incineration of solid waste are some sources of anthropogenic particles. The diversity of emissions presents a wide range sizes, concentrations and compositions of particles. And their size range spans several orders of magnitude, ranging from nanometers to hundreds of micrometers. Similarly, the concentrations might be from 1.0^{7} to 1.0^{-6} particles per cubic centimeter. In addition, the particles in the atmosphere undergo processes that transform their physical and chemical properties. Therefore the study of atmospheric particles is complicated. However, an important tool in particles analysis is the construction of size distribution graphs. These charts provide relevant information such as the nature of the particles (i.e., maritime, continental, urban, or rural zones), because each place has a kind of specific particle sources.

In the study we use particle size distributions from inside, outside and away from the clouds to identify and analyze possible changes of particles properties interacting with cloud droplets. Particle counters at the C130 aircraft provided the information. The instruments measure aerosol particles and cloud droplets in different size ranges and cover a wide range of sizes (~ 0.1 to 50 microns).

The PCASP dehydrates particles reducing the relative humidity below 30%, but the FSSP measure them at ambient relative humidity, so we calculate the dry particle diameter from both FSSP, based on the Tang's theory (1976) and Tang and Munkelwitz (1977), to obtain a size distribution of dry particles.

3.2. Interaction between particles and clouds

There are four main processes involved in the interaction particles-clouds:

a. Vertical distribution

The classic physics model for developing convective clouds indicates that the aerosol particles are incorporated from the base of the cloud. Some particles form droplets that grow vertically while being transported by updrafts currents generated by latent heat during a phase change from vapor to liquid. A few drops reach the top of the cloud, where updrafts currents lose strength by neutral stability between the cloud and the environment. At this point, the interaction of clouds with dry air dilutes and evaporates drops. In this mixing and evaporation zone of droplets is where the particles, used as CCN to form cloud droplets, are released back into the upper top of the cloud reaching the high troposphere and in some cases of deep convection may lead them to the lower stratosphere. Some researchers have shown that this mechanism is the main transport of particles from the boundary layer to free troposphere (i.e., Flossmann, 1998).

b. Mass incorporation into the drop by diffusion

A particle in a high relative humidity environment will grow by diffusion and condensation of vapor molecules producing a cloud droplet. The particle can be diluted to form a solution within the droplet. In that case, if the droplet is in an atmosphere of various gases that can be absorbed by the same specie (i.e., SO_2 in marine clouds) there is an increase in the mass concentration of solute within the droplet changing its physical properties (mass increase). A rapid change in pH also transform the chemical properties, resulting in the dissolution of species in a solution (Hegg and Hobbs, 1982; Leaitch, 1996; Leaitch et al, 1986, O'Dowd et al, 2000).

When a particle is in high relative humidity (~ 80%) environment, it becomes an effective site for oxidizing species in aqueous phase (Chameides and Stelson, 1992). For example, SO_2 dissolved in a particle can react with ozone and hydrogen peroxide. In an acid particle (H_2SO_4) with low pH, the oxidant is hydrogen peroxide, but for particles with high pH (i.e., $[NH_4]_2SO_4$), the oxidant will be ozone. The first reaction is more important in maritime areas, because SO_2 is abundant from dimethyl sulphide emissions produced by phytoplankton. O'Dowd et al, (2000) estimate that under mass incorporation conditions a particle can increase its size to double in about 400 seconds.

c. Collision-coalescence of drops

When the droplets have certain size, they grow more efficiently by collision-coalescence. The collision and coalescence among cloud droplets is mainly governed by gravitational effects, so large droplets fall faster than small ones. This process produces a decrease in the concentration of drops, but form larger particles and evaporate the droplet mass. Each collision-coalescence between two original CCN becomes in to one drop, which has a mass equal to the sum of the two nuclei. If the original CCN have a different composition, it also changes the chemical composition of the resulting drop.

d. Mechanical removal

The removal of particles by precipitation is a cleaning process from the atmosphere. This mechanism helps to maintain a balance between sources and sinks of particles. The precipitation removes mechanically particles by inertial collection and transportation of raindrops, and also removes the nuclei when the drops become rain. However, it depends on the size of the interstitial space of the particles, related to the size of the drop. Experimental studies of Chate et al, (2003) demonstrated that this mechanism is more efficient on particles in the range of coarse mode (> 1 μm). Other studies have also shown that removal by inertial collection and transportation only affects to a small percentage of particles that are on base of the cloud (Wang and Pruppacher, 1977).

3.3. Mechanisms of interaction between particles and clouds

The mechanisms that modify the properties of atmospheric particles are varied and have different efficiencies depending on the size of the particles. The size distribution and the area plots of particles in the study showed four patterns that may be associated with processes of interaction between particles and clouds:

1. Vertical transport with mixing and dilution with minimum changes in the size
2. Aqueous phase oxidation of aerosol precursors (≤ 1 micron)
3. Droplet coalescence (> 1 micron)
4. Removal by precipitation

Charts on figure 3 illustrate the general features that are described as follows:

1. Vertical transport with mixing and dilution

This cloud processing mechanism, discussed in detail by Flossman (1998), transports particles from cloud base to upper regions of the cloud where they eventually are detrained, either at cloud top edges or by mixing with ambient aerosols at detrainment level. PSD signatures take one of two forms. If RH at the point of measurement is higher than RH at cloud base, then PSD exhibits a tail at larger sizes exceeding that of the cloud base PSD (Fig. 3, pattern A1). Other studies have shown the correlation between RH and changes in particle size near cloud boundaries (e.g., Baumgardner and Clarke, 1998). This, or the particles have mixed with air close of to the same RH as at the cloud base so that the resulting PSD is one that has approximately the same shape as at cloud base, but with lower concentrations as a result of the dilution with ambient air (Fig. 3, pattern A2).

2. Aqueous phase oxidation of aerosol precursors

In-cloud oxidation of dissolved species is a process that increases the mass of aerosol particles and may change their composition (Hegg and Hobbs, 1982; Leaitch, 1996; O'Dowd et al., 2000). The likely precursor gas in the EPIC research region is SO_2, which evolves from dimethyl sulfide produced by phytoplankton or from anthropogenic sources, as discussed below. The PSD pattern produced by this process will be indistinguishable from pattern A unless additional information is known about the aerosol chemistry. As discussed in section

2.4, measurements were not made for particle composition, but the average refractive index of particles could be estimated. A comparison of the average refractive index at cloud base with the near-cloud and far-cloud values at higher altitudes suggest changes in particle composition, as shown in Fig. 3 where the cloud base refractive index is near that of sea salt (1.54), while the near-cloud value at 2500 m is closer to that of ammonium sulfate (1.48). The observed differences are based on a technique that has a large amount of uncertainty and is used qualitatively in the present study as an indicator of composition change.

3. Droplet coalescence

Coalescence decreases the number concentration of particles while shifting the mass to large sizes. Each coalescence event decreases the number of original CCN by one and the resulting mass is the sum of the two nuclei. If nuclei are of different composition, then this process also changes the chemistry of the particle contained in the resulting drop. The large particle mode, with a peak between 5 – 6 μm, seen in Fig. 3 indicates coalescence, since neither the cloud base nor far-cloud PSD have particles in this size range.

4. Removal by precipitation

Precipitation removes particles mechanically by inertial or nucleation scavenging when cloud droplets become raindrops. Mechanical scavenging depends on the size of interstitial aerosol in relation to the raindrop size. Experimental results (Wang and Pruppacher, 1977) suggest that only a few percent of the interstitial and sub-cloud particles are removed by this mechanism and this is not considered as a major factor here. The majority of aerosols removed by precipitation will be those that are in cloud droplets growing by condensation and coalescence to precipitable sizes. Figure 3 illustrates this process where PSDs at the cloud base level are quite different depending upon whether the measurements were made at the actual cloud base or in the far-cloud air. The far-cloud PSD has particles of super-micron sizes, but such particles are noticeably missing at the cloud base. In this particular case, the cloud base measurements were made after the cloud had formed and the super-micron particles had been activated and grew quickly to droplet sizes that could coalesce and precipitate.

4. Analysis and discussion

Five flights and ten cloud systems were selected for analysis based on a visual evaluation of the records made with the forward- and side-looking video cameras on the aircraft. The criteria was that no other clouds could be seen within around 10 km on either side of a cloud line, such that far-cloud samples represent “ambient” aerosols, i.e., lacking any recently processed particles by clouds.

4.1. Time series to identify clouds

We studied the data from flights 7, 9, 12, 13 and 17. The flights were conducted in convective clouds by passing through the clouds at different levels (1000, 2500, 4200, and 6000 meters). Moreover, we passed through the cloud base (300 meters) and at surface level (30 meters).

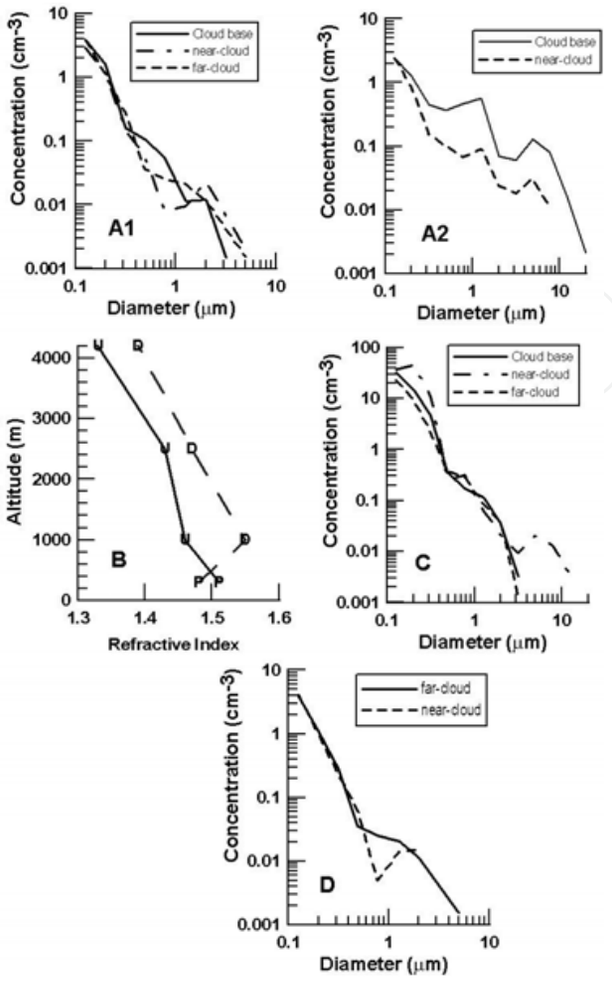


Figure 3. Cloud processing signatures

Furthermore, during the flights were conducted surveys of the atmosphere's vertical profile. This information is useful because surveys have different locations, but they are associated to the clouds recorded data.

We observed changes in the properties of atmospheric particles and the processes responsible. Also we recorded environmental and weather conditions in zones which the property changes occur more frequently, comparing both sides of the clouds.

The droplets concentration in a cloud is function of the particles number in the atmosphere, so any variation in the amount of particles will affect the cloud microphysics evolution. In marine areas the concentration of particles is about 100 per cm^3, if there is a greater amount of particles is likely to pollution particles are present. The EPIC 2001 research area is located approximately 800 - 1000 km away from Mexico and Central America, allowing the transport of pollutants from the continent to the area when the prevailing winds are favourable. The opposite situation is also possible in maritime areas away from the coast. Wind patterns during flights 12 and 13 shows weather characteristics of maritime areas.

The cloud boundaries are identified by means of videotapes taken from the plane C-130 and the analysis of time series using reference measurements obtained by the FSSP100. The

criterion was to consider the instrument's concentration records ≥ 1 cm^{-3} obtained within the cloud. In EPIC 2001, we identified 10 cloud systems that met the minimum information necessary for the study. Table 2 shows the location, date and time of each cloud systems. The data correspond to the average information of all transects made to the system.

						300 m						4200 m					
Flight #	Date 2001	Cloud System	Time Period (UTC)	Location	Particle Source	CN Conc (cm^{-3})	PCASP Conc (cm^{-3})	Cloud base length (m)	Cloud base T (°C)	Cloud base wind speed ($m\ s^{-1}$)	Cloud base RH (%)	Cloud top length (m)	Cloud top T (°C)	Cloud top wind speed ($m\ s^{-1}$)	Cloud top RH (%)	CN Conc. (cm^{-3})	PCASP Conc (cm^{-3})
7	sep-16	1	16:46-17:19	12.3°N, 93.7°W	HG	910	345	4800	25.60	1.4	79	***	***	***	***	***	***
7	sep-16	2	18:42-20:12	11.9°N, 95.2°W	HG	830	227	25740	25.04	2.5	80	13900	2.44	9.3	91	3370	447
9	sep-20	3	18:16-20:11	10.5°N, 95.9°W	MR	380	66	18093	24.18	1.3	85	500	3.63	0.3	65	320	32
9	sep-20	4	18:56-20:24	8.2°N, 95.8°W	MR	200	40	12860	23.63	1.5	83	2640	2.95	3.4	79	810	48
12	sep-28	5	17:03-18:12	9.3°N, 93.9°W	MR	460	138	13970	25.26	3	83	680	3.7	7.2	62	590	32
12	sep-28	6	19:14-20:20	11.9°N, 94.1°W	MR	420	143	4550	24.87	1.2	80	7040	3.74	2.7	80	818	14
13	sep-29	7	18:31-19:03	11.4°N, 94.6°W	MR	360	98	11440	24.06	1.6	84	2970	3.97	1.9	88	15574	50
13	sep-29	8	19:36-20:22	12.4°N, 94.9°W	MR	390	64	9460	24.15	1.5	84	8690	3.88	2.7	85	1119	98
17	06-oct	9	18:34-19:49	11.9°N, 93.9°W	HG	1900	696	36200	26.02	2.3	82	5060	3.92	5.8	81	2810	384
17	06-oct	10	20:51-21:36	11.8°N, 94.1°W	HG	1600	510	10560	26.53	0.9	68	2480	3.2	2.4	72	1080	350

Table 2. Characteristics of cloud system selected for the analysis

Flights 9, 12, and 13 were made on days with "maritime" (MR) aerosol background and when winds came from the southwest. "Higher" (HG) aerosols concentrations correspond to flights 7 and 17 with average concentrations significantly higher than the other three flights. Table 2 summarizes the time, location and type of cloud systems.

4.2. Cloud boundaries comparison

A convective cloud in its formative stage has a rapid vertical development. The ambient air surrounding the cloud incorporates into the cloud increasing its volume with the vertical expansion. This process is known as entrainment, so its mixing process is more efficient outboard in the cloud with sub-saturated air from the environment. The droplets evaporate and particles served as CCN are released back into the atmosphere. The mixing with ambient air and the evaporation of cloud droplets produces a cooling air parcel which generates a negative buoyancy force. This could result in shear zones, as the turbulence caused by this effect helps to mix ambient air with the cloud and evaporate more drops. To define the distance corresponding to the cloud border, we did a time series properties analysis of the particles in the clouds, to evaluate the zone of influence. Figure 4 shows the changes in properties of the particles in the vicinity of the cloud. The area of influence for the interaction of particles with the cloud covers a distance of approximately 500 m from the cloud's border. The FSSP100 drops concentration

measurements correspond to the solid line, which marks the cloud's boundary. Each tick mark represents 110 m at the aircraft's average velocity of 110 m s^{-1}. The dotted lines represent the behavior of the average diameter of particles measured by the FSSP300 (dash) and FSSP100 (dash and dot). These values denote the limits of the transition region between ambient and cloud air. Diameter measurements show a significant increase of particles up to ~500 m from the cloud's boundary. That determines the representative area to evaluate the mechanisms that modify the properties of particles due to the interaction with the cloud.

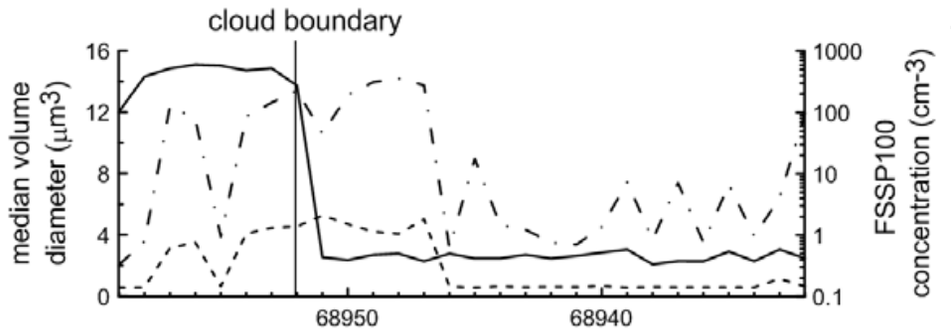


Figure 4. Medium volume diameters measured by FSSP300 (dashed line) and FSSP100 (dot-dash line) indicating a cloud boundary.

The particles properties on both sides of the cloud border must be different. The particles characteristics in the neighboring area of the cloud have a determining effect on the modification of some of their properties. Changes in humidity, altitude and environmental conditions, where the samples are collected, affect the particles concentration and size. So, in order to compare both sides of the cloud we analyze data from the clouds vicinity (500 m from the border of the cloud) to obtain average values. Figure 5 shows the average concentrations of vertical profiles measured by the PSCASP (> 0.1 microns) on the cloud borders (cases identified by U, D or P). A third profile, corresponding to a far area from the cloud (average 500 to 1500 m from the border (dotted line), is used to compare the profiles against those close to the cloud.

In conditions with and without pollution, particle profiles measured in the vertical gradient has two patterns. One shows a constant value or a decrease with height. The second shows an increase in concentration up to 2500 m and then decreases to lower values than those measured at the base. It is possible to observe cases where the particle concentration profiles are similar to the concentration profile far away from the cloud. This is due to the presence of dilution processes, where particle concentrations in the vicinity of the cloud are lower than in remote areas. When the concentration of particles near the cloud is greater than the environment it is possible that there is an increase of particle size < 0.1 μm to ranges that is not possible to detect. In summary, measures of concentration of particles increased with height indicating that the smaller particles (< 0.1 μm) at the base of the cloud grow to detectable size ranges for the instrument during transport through the cloud. On the other hand, when the concentrations decrease with height means a dilution effect.

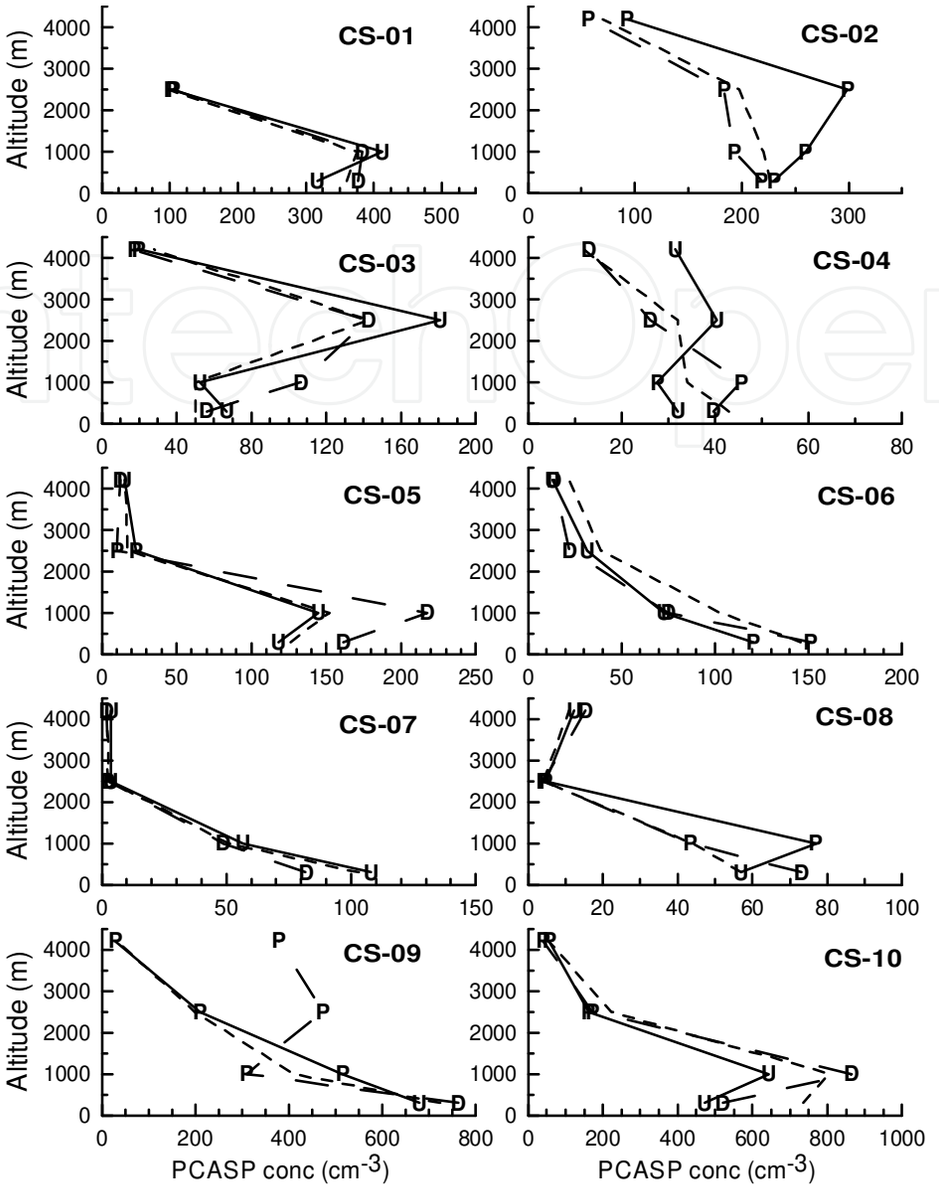


Figure 5. Vertical profiles of particle concentrations measures for the 10 cloud cases. The far-cloud profiles (short dashed) and near-cloud profiles on each side of the cloud (solid and long dashed lines).

Figure 6 shows concentrations measured with FSSP100 (> 2 μm) in the vicinity of the cloud (solid and dotted lines) and away from the cloud (dotted line). In the region where there are drops of cloud measurements, we used them to detect giant particles (> 1 micron) coming from the ocean. In most cases, the concentration values for particles greater than 1 micron near the cloud have a maximum at 1000 m high. It happens perhaps because smaller size particles increased their volume within the cloud.

Sometimes it is possible to observe when the particle concentrations decrease with height that there is an increase in the concentrations of larger diameters. The combination of patterns is indicative of changes in particles by mixing and dilution on the total concentration dominated by small particles. Also, a simultaneous increase in the concentrations of particles suggests that it there is a change in particles size.

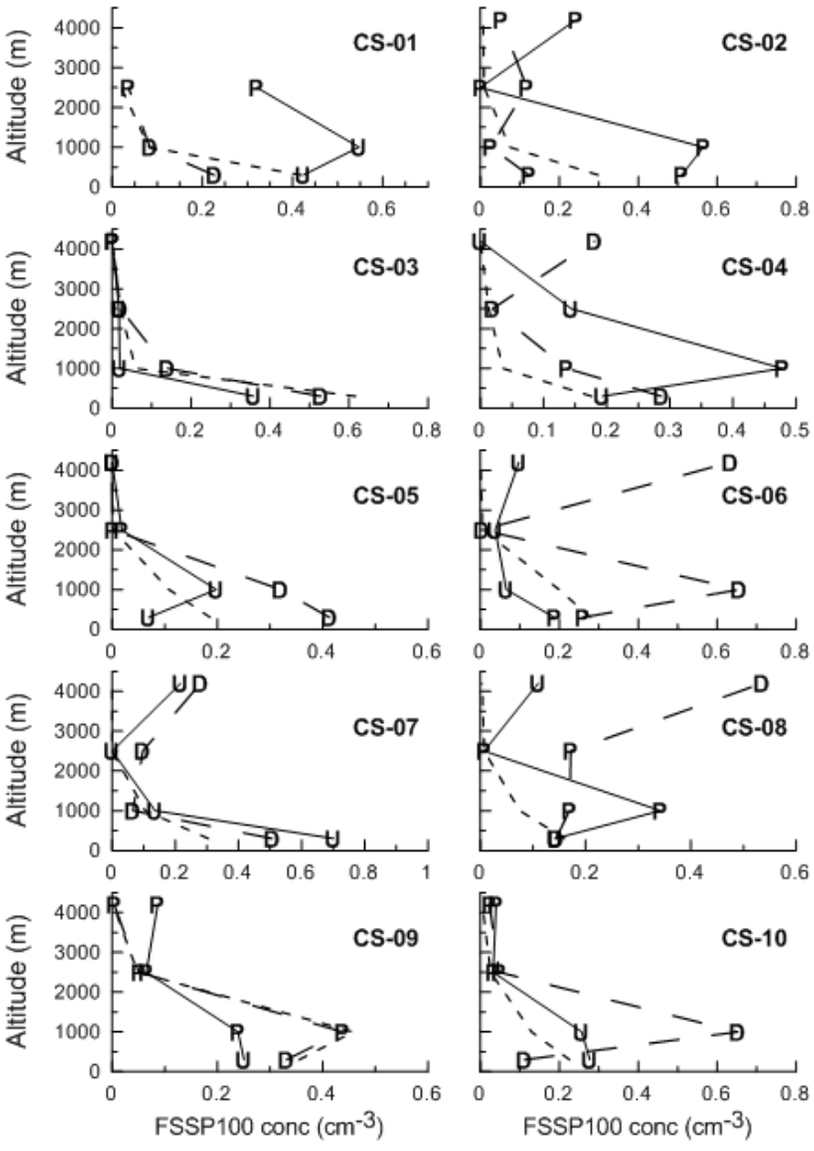


Figure 6. The vertical profiles of concentrations measured with the FSSP-100.

4.3. Processes classification and evaluation

There are different processes at each side of the cloud and in each level of each clouds system. We used as reference the processes signal description and their property. This subjective classification is based on an examination of vertical profiles, shown in Figs. 4, 5, and 6 and on the shapes of PSDs associated with the near-cloud region at each level. The 300 m passes were only evaluated for evidence of removal by precipitation (pattern D). Figure 7 summarizes the frequency of each category. There were 49 classifications made on MR days and 35 during HG days. A classification could not be made in 10% of the MR cases and 5% of the HG ones. The largest fraction of the observations was classified as pattern A (40% and 60% of MR and HG cases, respectively). Pattern C matched only 4% of the MR observations and none during HG days. Patterns B and D were equally represented during both MR and HG days.

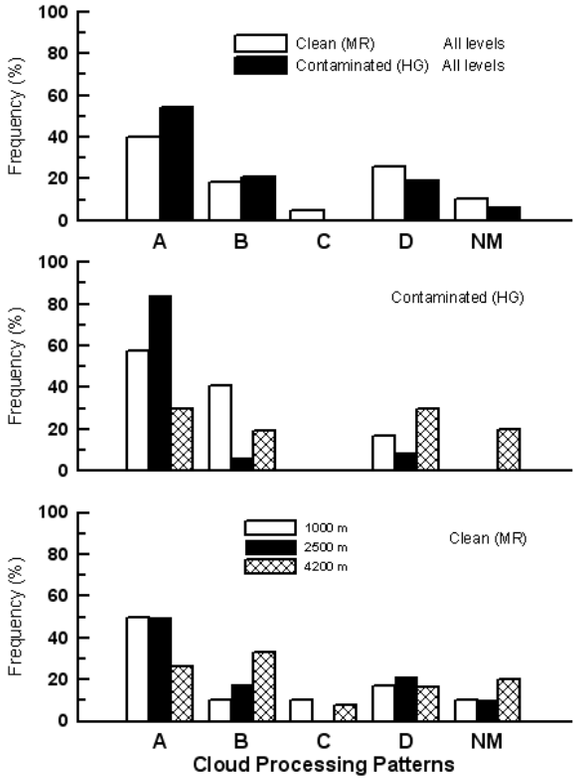


Figure 7. Percentages of cloud processing signatures, derived from vertical profiles of particle properties and evaluation of particle size distributions, for the MR cases (bottom panel), HG cases (middle), and combined cases.

There were no consistent trends with altitude between MR and HG days. Particles at 1000 m and 2500 m altitude were predominantly like pattern A, in both the MR and HG cases. In MR cases, there were slightly more type B than type A particles at 4200 m. In HG cases, the 4200 m particles were evenly distributed between patterns A and D.

4.4. Particle composition estimation

The refractive index was used to estimate the particles composition at the ends of the clouds. We calculated and average refractive indices at 500 m from the borders of the cloud. Figure 8 shows the results. The refractive index profile for the area between 1000 and 1500 m away from the border of the cloud is also shown. This area is considered free from the influence of particle processing by clouds.

We consider three refractive indexes as benchmarks. The refraction indexes of water (1.33), ammonium sulfate (1.48), and sodium chloride (1.54). Another factor we take into account is the size distribution and composition of particles as a function of their height in normal conditions without the influence of pollution. The type and composition of particles depend on local sources. Thus, in sea areas the main sources are the production of salt particles from the surface of the oceans that are caused by wind friction and breaking waves. These particles are mainly in the lower parts of the troposphere near its source. In the upper troposphere, main sources of particle are the conversion of gas to particle and deposition by

clouds (Hobbs, 1993) which produce small particles (< 0.1 μm). In marine areas the particles are composed of sulfate, because they are formed by the condensation of SO_2. Particles ranged between 0.1 to 1 microns are composed of sulfate (Hobbs, 1993). Based on the sources we expected to find high ammonium sulfate in the lower troposphere.

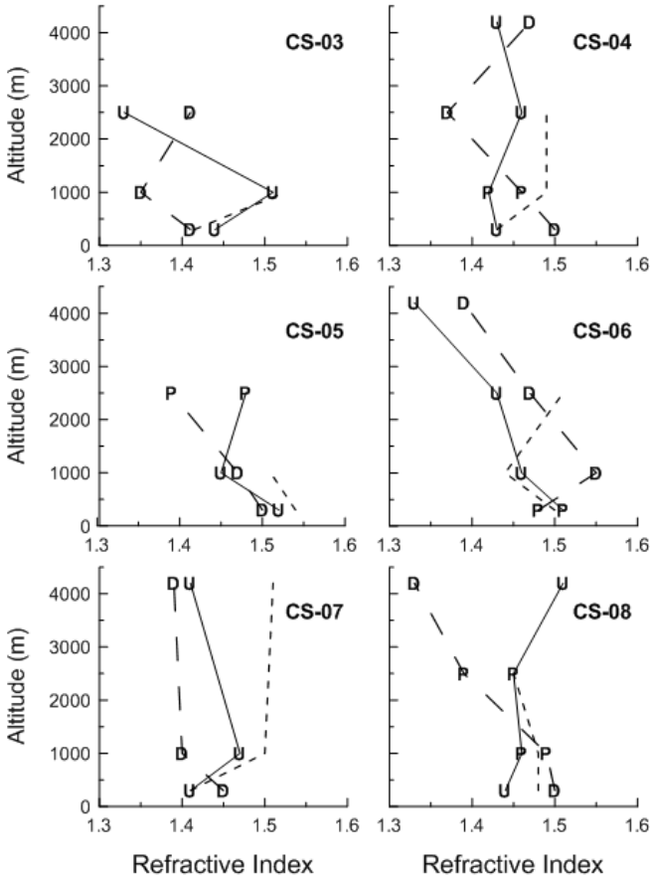


Figure 8. Derived refractive indexes for far- and near-cloud vertical profiles for the maritime (MR) day cases.

In estimating the composition of particles from optical counters measurements, the environmental conditions can strongly influence the outcome. Figure 9 shows the comparison between the dispersion coefficients obtained with a nephelometer and the dispersion coefficient calculated from the particles size distribution. Data were collected on transects at 2500 m without pollution (Figure 9 right) and with pollution from the continent (Figure 9 left). The reference line 1:1 is used to compare dispersion coefficients calculated and from nephelometer, assuming three different compositions.

Figure 9 (left) shows that polluted cases at the same height had calculated coefficients higher than those measured with instrumentation. This may be due to anthropogenic particles that absorb and scatter light. So, the measured values will be lower than calculated, since it is not taken into account the particles absorption. Moreover, no polluted cases have a better correlation because marine particles do not absorb light. This feature allows us to use this technique to more easily estimate the composition of particles in cases without contamination.

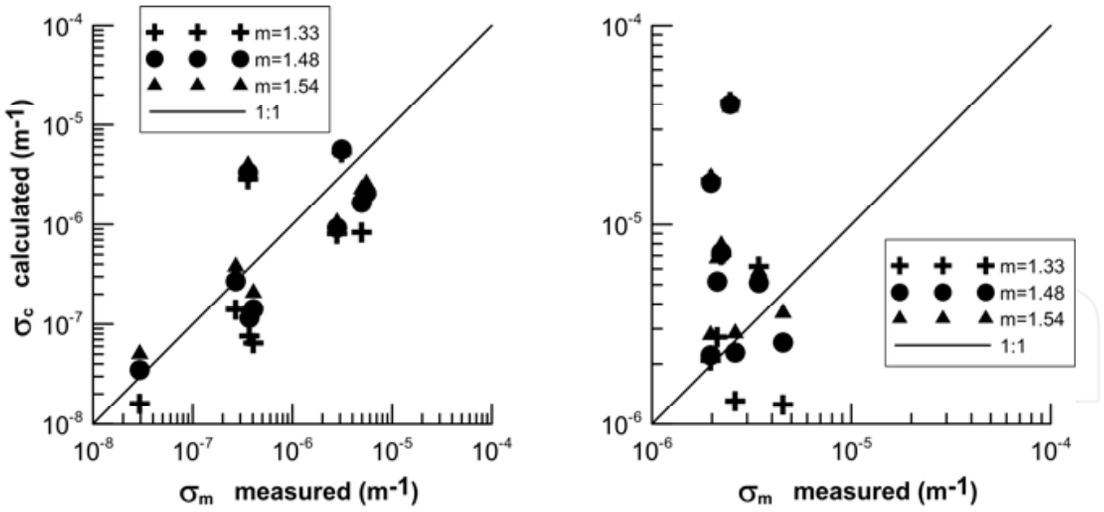


Figure 9. Scattering coefficients compared against those measured with the nephelometer for three refractive indexes: 1.33, 1.48, and 1.54, for MR days (a) and high aerosol concentrations (HG) days (b).

5. Effects of atmospheric particles

Atmospheric particles play an important role in the planet radiative budget. Their effects on radiative forcing by absorbing solar radiation backscattered or as facilitating clouds formation are important objects of study.

The uncertainty of particle-radiation interactions is still very large. For example, some particles with sulfate or organic carbon cool the atmosphere. On the other hand, black carbon particles warm it, because they absorb visible light and convert it into thermal energy (IPCC, 2000). This strange balance increases the uncertainty of the magnitude of their effects on the atmosphere.

5.1. Direct effects of particles processed by clouds

The cloud process and modify particles size and composition. Larger particles scatter more sunlight and increase the extinction of light. This impact on the radiative balance can be estimated with the optical depth, since the extinction of particles is expressed:

$$\boldsymbol{\tau(\lambda) = \int_0^\infty \sigma_e(\lambda, z)dz} \quad (3)$$

Where τ is the optical thickness and σe is the particle's extinction coefficient. In our case, we assume that the particle's composition is mainly sodium chloride (sea salt) and sulfates. The particle does not absorb visible light, so its extinction and dispersion coefficients are equal. Thus, the above equation becomes:

$$\boldsymbol{\tau = \sum_{n=30}^{4200} \sigma_{s(n)} \Delta z} \quad (4)$$

To calculate the optical depth, we use the size distribution spectra for the following heights: 30, 300, 1000, 2500 and 4200 m on both sides of the cloud, as well as the average between 1000 and 1500 m away from the cloud.

Table 3 shows the optical depth on both sides of the cloud (upwind and downwind) and data away from the cloud that are used as reference atmosphere without the influence of processed particles. The values are higher near than far away from the cloud. Figure 10 shows the optical depth near and far from the cloud. The particle optical depth near the cloud is 10 times higher than distant to the cloud. System 7 has a ratio about 1:1 indicating that the physical and optical properties of particles near and far from the cloud do not exhibit noticeable differences. The data suggest that particles near to the cloud in system 7 have not been yet processed or it could be a very young cloud with no mixing with ambient air.

cloud	τ (U)	τ (D)	τ (far)
1	0.125	0.021	0.027
2	0.158	0.373	0.018
3	0.116	0.124	0.013
4	0.152	0.196	0.017
5	0.192	0.118	0.010
6	0.247	0.316	0.084
7	0.171	0.231	0.211
8	0.272	0.306	0.005
9	0.322	0.355	0.036
10	0.196	0.613	0.041

Table 3. Optical depth on both sides of the cloud

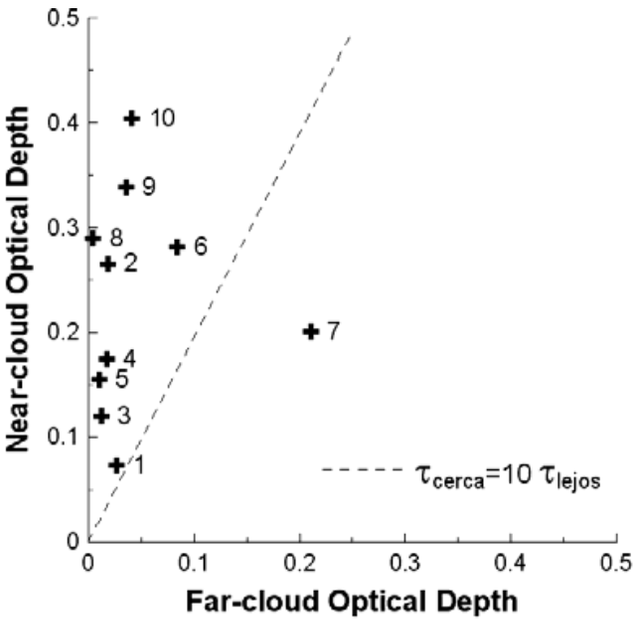


Figure 10. Optical depths calculated for particle size distributions at 30, 300, 1000, 2500, and 4200 m, near-cloud and far-cloud cases. These optical depths are compared for the ten cases (labeled by their number).

The decrease in the amount of radiation reaching Earth's surface can increase the optical depth, suggesting that cloud particles processed promote a local cooling. Indeed, satellite images of cloud cannot detect the optical depth because it is very large.

5.2. Indirect effects of particles processed by clouds

Five flights and ten cloud systems were selected for analysis based on a visual evaluation of the records made with the forward- and side-looking video cameras on the aircraft. The criteria was that no other clouds could be seen in 10 km on either side of a cloud line, such that far-cloud samples represent "ambient" aerosols, i.e., lacking any recently processed particles by clouds. Flights were also classified by aerosol type. Figure 11 shows frequency distributions of CN and PCASP measured concentrations at ≤ 300 m for those five days. Flights 9, 12, and 13 were made on days with "maritime" (MR) aerosol background and when winds came from the southwest. "Higher" (HG) aerosols concentrations correspond to flights 7 and 17 with average concentrations significantly higher than the other three flights. Table 2 summarizes the time, location and type of cloud systems.

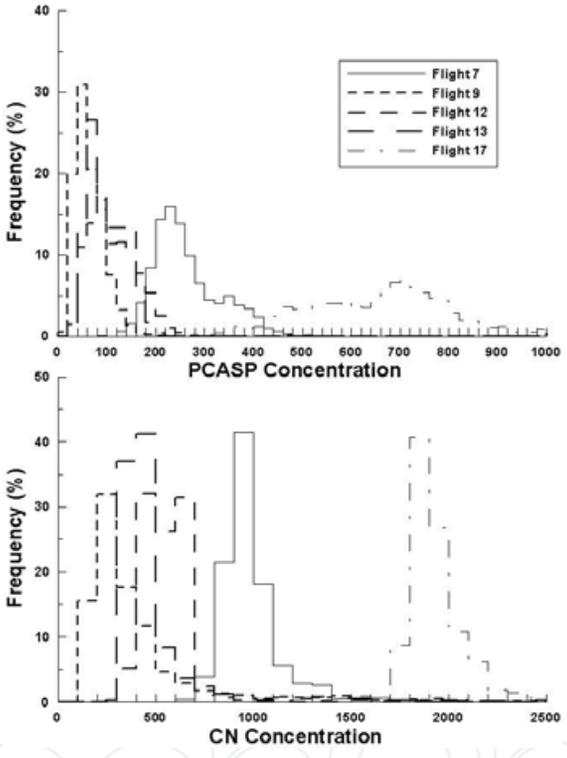


Figure 11. The frequency of occurrence of 300 m concentrations measured by the PCASP (top panel) and CN (bottom) are shown here for the five days used in the case studies.

The cloud albedo depends on the concentration of droplets (Twomey, 1974). One way to estimate, with good approximation, the changes in albedo (A) is using the Meador and Weaver (1980) equation:

$$A = \frac{(1-g)\tau}{1+(1-g)\tau} \tag{5}$$

Where g is the asymmetry factor, which is the average cosine of scattering angle. For the scattering clouds by sunlight g = 0.85 (Hobbs, 1993), we can simplify the equation 5.3 to:

$$A = \frac{\tau}{\tau+6.7} \tag{6}$$

The cloud optical depth (τ) of h that contains a concentration of droplets n (r), with radius r is given by:

$$\tau = \pi h \int_0^\infty Q_e r^2 n(r) dr \quad (7)$$

Where Qe is the extinction efficiency factor for the wavelengths of visible radiation (λ = 400 – 700 nm).

We calculated the single scattering albedo employing equations 5.4 and 5.5 for each concentration of drops at 6000 m, using a layer of cloud thickness h = 100 m, based on the distance of a datum to another along the horizontal axis (data per second). The 6000 m level is considered the top of the ice-free clouds. Previous figure shows the histograms of the single scattering albedo calculated inside the cloud for different environmental conditions. The albedo on HG episodes ranged between 0.8 – 0.9, while in MR days ranged between 0.6 – 0.8. The results agree with those obtained theoretically by Lohmann et al (2000) stating that anthropogenic pollution causes a diminution in the effective radius of cloud droplets and an increase in the albedo of the cloud.

There is a relationship between the maximum concentrations registered by both FSSP100 and PCASP, indicating a higher concentration of cloud droplets in the episodes with anthropogenic influence and resulting in a diminution in droplet size, because a bigger amount of CCN compete for moisture in the air. Last figure shows the different droplets average diameters in pollution-free days (~14 microns) and polluted days (~10 microns).

Analysis shows the indirect effect of the particles in the formation of convective clouds. During episodes of anthropogenic contamination, the concentration of droplets in the cloud increases and their size decrease, thus causing low rainfall. These phenomena will increase the albedo of the cloud, because it depends on the concentration of drops (Twomy, 1974).

Table 4 shows the values of optical depth (τ) and albedo (A) of the clouds studied. The highest values of albedo were presented in systems 1 and 9, corresponding to days with pollution.

Cloud	τ	Albedo
1	66.46	0.63
2	27.35	0.46
3	31.75	0.42
4	29.38	0.52
5	34.04	0.49
6	65.48	0.58
7	37.29	0.53
8	43.28	0.52
9	165.90	0.73
10	40.18	0.54

Table 4. Optical depth (τ) and albedo (A) of clouds studied

6. Conclusions

The physical and optical properties analysis of atmospheric particles is focused on the observation of several processes involved in convective clouds and their environment. We have studied cloud systems on Mexico's Pacific ITCZ. The research flights were conducted during September and October 2001. The data obtained point to some relevant cases marked by the weather and cloud characteristics. The analysis and evaluation of information allows us to reach the following conclusions.

We identify the most important interaction processes between particles and clouds, which can cause changes in the size and composition of atmospheric particles: a) diluting the concentration of particles with minimal changes in size, b) increasing atmospheric concentration of submicron particles (≤ 1 μm), c) increasing the concentration of atmospheric supermicron particles (> 1 μm) d) removal of supermicron particles. The analysis of particles and clouds interaction shows that the most common contact mechanisms were: a) vertical transportation with mixing and dilution, which occurred in 44% of the MR days and 55% on HG episodes b) oxidation of aqueous phase particles are present in 20% and 24% days MR and HG events, respectively, c) coalescence of droplets occurred in 18% and 15% days MR and HG, respectively.

The particles change their optical properties and the way they interact with solar radiation and clouds. Particles that are processed in the vicinity of the cloud increase the optical depth. The growth comes in quantities up to 10 times larger than the value recorded in distant particles. Therefore, variations in the optical properties of particles affect directly the radiative balance and influence in local climate.

The cloud observations were classified into two categories: typical values of maritime areas with prevailing westerly winds and low concentrations of cloud condensation nuclei (conc. < 500 particles per cm^3) and values influenced by anthropogenic pollution (conc. < 1800 particles/cm^3).

Increasing the concentration of particles in a place influenced by a pollution source also enlarged the number of CCN. Data analysis shows a good correlation between the concentration of CCN at cloud base and the concentration of droplets inside the cloud (r^2 = 0.92), which explains the clouds albedo augmentation on days with influenced by anthropogenic pollution.

Future work considers the application of detailed microphysics models to evaluate the different processes of interaction of particles and clouds. Thus, also intends to use these models to analyze the effect of these particles processed in the dynamics of the cloud as well as the influence on processes like rain.

Author details

J.C. Jiménez-Escalona
ESIME U. Ticomán, Instituto Politécnico Nacional, Gustavo A. Madero, Mexico City, Mexico

O. Peralta
CCA, Universidad Nacional Autónoma de México, Ciudad Universitaria, Mexico City, Mexico

7. References

Albrecht B.A., 1989, Aerosol, cloud microphysics, and fractional cloudines, Science, 262, 226-229.

Alfonso, L. and G.B. Raga, 2002: Estimating the impact of natural and anthropogenic emissions on cloud chemistry. Part I: Sulfur cycle. Atmospheric Research, 62, 33-55.

Baumgardner D., Cooper, W.A., Radke, L.F., 1996, The interaction of aerosols with developing maritime and continental cumulus clouds, 12th Int. Conf. on Clouds and Prec. Zurich, 308-311.

Baumgardner, D., Clarke, A., 1998, Changes in aerosol properties with relative humidity in the remote southern hemisphere marine boundary layer. J. Geophys. Res., Vol.103, No. D13, 16,525-16,534.

Chameides, W.L., Stelson, A.W., 1992, Aqueous phase chemical processes in deliquenscent sea-salt aerosol: a mechanism that couples the atmospheric cycles of S and sea-salt, J. Geophys. Res. 97, 20565 – 20580.

Charlson R.J., Schwartz S. E., Hales J.M., Cess R.D., Coakley J.A., Hansen Jr J. E., Hofmann D.J., 1992, Climate forcing by anthropogenic aerosols, Science, Vol. 255, 423–430.

Chate D. M., Rao P.S.P., Naik M.S., Momin G. A., Safai P. D., Ali K., 2003, Scavenging of aerosols and their chemical species by rain, Atmos. Environ, 37, 2477 – 2484.

Coakley J. A., and Grams G., 1976, Relative influence of visible and infrared optical propierties of a stratospheric aerosol layer on the global climate, J. Appl. Meteorol., 15, 679 – 691.

DeFelice T. P., Saxena V. K., 1994, On the variation of cloud condensation nuclei in association with cloud systems at a mountain-top location, Atmos. Res., 31, 13-39.

DeFlelice, T.P., Cheng, R. J. 1998, On the phenomenon of nuclei enhancement during the evaporative stage of a cloud, Atmos. Res., 47-48, 15-40.

Delene D.J., Deshler T., Wechsler P., Vali G., 1998, A ballon-borne cloud condensation nuclei counter, J. Geophys. Res. 103 (D8), 8927–8934.

Delene D.J. and Deshler T., 2000, Calibration of photometric cloud condensation nucleus counter designed for deployment on a balloon package, J. Atmos. Oceanic Tech, 17(4):, 459-467.

Emanuel, K. A., 1982, Inertial inestability and mesoscale convective systems. Part II: Symmetric CISK in a baroclinic flow. J. Atmos. Sci. 39, 1080-1097.

Flossmann, A.I., 1998, interaction of Aerosol Particles and Clouds, J. Atmos. Sci., Vol 55,879-887.

Hansen J. E., et al., 1980, Climatic effects of atmospheric aerosols, Ann. New York Acad. Sci., 338, 575 – 587.

Hegg D. A., Hobbs, P.V., and L. F. Radke, 1980, Observations of the modification of cloud condensation nuclei in wave clouds, J. Rech. Atmos, 14, 217-222.

Hegg D. A., Hobbs, P.V., 1982. Measurements of sulphate production en natural clouds. Atmos. Environ., 2663 – 2668.

Hobbs, P.V. 1993: Aerosols-Cloud Interactions, Aerosol-Clouds-Climate Interactions, Academic Press. pp. 33-73

Holton J. R., 1992, An introduction to dynamic meteorology, Academic Press, 507 pp.

Hudson, J. G., 1989: An instantaneous CCN spectrometer. J. Atmos. Ocean. Technol.,6, 1055-1065.

Jiménez-Escalona J.C. and Peralta O, 2010. Processing of aerosol particles in convective cumulus cloud: a case study in the Mexican east pacific, Advances in Atmospheric Sciences, Vol. 27, No. 6, pp 1331 – 1343.

Leaitch, W.R., Strapp, J.W., Wiebe, H.A., Isaac, G.A., 1986. In: Pruppacher, H.R., Semonin, R.G., Slinn, W.G.N. (Eds.), Precipitation Scavenging, Dry deposition, and Resuspension. Elsevier, pp. 53 - 59.

Leaitch, W.R., 1996. Observations pertaining to the effect of chemical transformation in cloud on the antropogenic aerosol size distribution. Aerosol Sci. Technol. 25, 157 – 173.

Lohmann U., Tselioudis G., and Tyler C., 2000, Why is the cloud albedo-particle size relationship different in optically thick and optically thin clouds?, Geophys. Res. Lett, 27, No 8, 1099 – 1102.

Meador, W.E. and Weaver, W.R., 1980, Two-Stream Aproximations to Radiative Tranfer in Planetary Atmospheres: A Unified Description of Existing Method and a New Improvement, J. Atmos. Sci, Vol 37, No. 3, 630-643

Mie, G., 1908: Beitrage zur optik trüber medien speziell kolloidaler metallösungen. Ann. Phys. 25, 377-445.

Naoki K., Hobbs P. V., Isjizaka Y., Quian G. W., 2001, Aerosol properties around marine tropical cumulus clouds, J. Geophys. Res. 106, D13, 14435–14445

O' Dowd, C.D., Lowe, J. A., Smith, M.H., 2000, The effect of clouds on aerosol growth in the rural atmosphere, Atmos. Res. 54, 201 –221.

Pollack J. B., et al., 1981, Radiative propierties of the background stratospheric aerosols and implications for perturbed conditions, Geophys. Res. Lett., 8, 26 – 28.

Pruppacher H. R. and Klett J. D., 1997: Microphysics of Clouds and Precipitation, Kluwer Academic Publisher., 954 pp.

Raga, G.B. and P.R. Jonas, 1993 a: Microphysical and radiative properties of small cumulus clouds over the sea. Quart. J. Royal Meteor. Soc., 119, 1399-1417.

Raga, G.B. and P. R. Jonas, 1993 b: On the link between cloud-top radiative properties and sub-cloud aerosol concentrations. Quart. J. Royal Meteor. Soc., 119, 1419-1425.

Rosenfeld, D., 1999: TRMM Observed first direct evidence of smoke from forest fires inhibiting rainfall. Geophys. Res. Letters, 26, 3105-3108.

Squires, P., 1958. The microstructure and colloidal stability of warm clouds. Tellus 10, 256-271.

Strapp J. W., Leaitch W. R., and Liu P. S. K., 1992, Hydrated and dried aerosol-size-distribution measurements from the particle measuring systems FSSP-300 probe and the deiced PCASP-100X probe, J. Atmos. Ocean. Technol.,Vol 9, No 5, 548-555.

Tang I. N., 1976, Phase tranformation and growth of aerosol particles composed of mixed salts, J. Aerosol Sci., Vol 7, 361 – 371.

Tang I. N., Munkelwitz H. R., 1977, Aerosol growth studies-III; Ammonium Bisulfate Aerosols in a moist atmosphere, J. Aerosol Sci., Vol 8, 321 – 330.

Twomey, S., 1974: Pollution and the planetary albedo, Atmos. Environ, 8, 1251-1256.

Twomey, S. 1991, Aerosols Clouds and Radiation, Atmos. Environ., 25A, 2435-2442.

Wallace J. M. and Hobbs P. V., 1977, Atmospheric Science, An introductory survey, 467 pp.

Wang, P. K. and H. R. Pruppacher, 1977: An experimental determination of the efficiency with which aerosol particles are collected by water drops in subsaturated air, J. Atmos. Sci., 34, 1664–1669.

Weller, B., B. Albrecht, S. Esbensen, C. Eriksen, A. Kumar, R. Mechoso, D. Raymond, D. Rogers, D. Rudnick, 1999: A science and implementation plan for EPIC: An eastern Pacific investigation of climate processes in the coupled ocean-atmosphere system. [Available online from http://wwwatmos.washintong.edu/gcg/EPIC/].

IntechOpen